

A Variable Heat Flux Model of Heat Transfer in Grinding: Model Development

T.-C. Jen

A. S. Lavine

Mechanical, Aerospace, and Nuclear
Engineering Department,
University of California, Los Angeles,
Los Angeles, CA 90095-1597

In any grinding process, thermal damage is one of the main limitations to accelerating the completion of the product while maintaining high quality. Therefore, the objective of the present study is to understand the thermal behavior in the grinding process and possibly achieve the ultimate goal of avoiding thermal damage in the grinding process. A model previously developed is improved to analyze the heat transfer mechanisms in the grinding process. Heat generated at the interface between the abrasive grains and workpiece (i.e., the wear flat area) is considered. A conjugate heat transfer problem is then solved to predict the temperature in the grinding zone. In the previous model, all the heat fluxes were assumed to be uniformly distributed along the grinding zone. This led to a contradiction in the temperature matching condition. This reveals that the heat fluxes into each of the various materials are not uniform along the grinding zone. An improved model, accounting for the variation of the heat fluxes along the grinding zone, is presented. The temperature and heat flux distributions along the grinding zone are presented, along with comparisons to previous theoretical results.

Introduction

The grinding process is an important precision machining process, which requires high accuracy. It is well known that this process requires a very high energy input in comparison to other machining processes (e.g., milling and turning). In any grinding process, virtually all the grinding energy is dissipated as heat in the grinding zone (Outwater and Shaw, 1952). Most of the heat generation in the grinding zone is due to friction and plastic deformation. This heat can cause the workpiece temperature to become elevated. Sufficiently high temperatures can cause various forms of thermal damage to the workpiece and wheel. Therefore, understanding the heat generation mechanism and the heat transfer paths are crucial in attaining the objective of avoiding thermal damage.

A substantial amount of research has been conducted on heat transfer in grinding. The interested readers are referred to Snoeys et al. (1978) and Malkin (1984) for detailed literature reviews. Some particularly relevant papers are reviewed here. A model was developed by Lavine and Jen (1991a), based on a series of previous studies (e.g., Lavine et al., 1989). The advantage of this model over earlier ones was that, by considering coupled heat transfer to the workpiece, wheel, and fluid, it eliminated the need to specify a priori the fraction of grinding energy entering the workpiece or the convective heat transfer coefficient of the grinding fluid. This model assumed that the heat fluxes into the workpiece, wheel, grains, and fluid were uniformly distributed in the grinding zone. However, an apparent contradiction for the temperature matching condition was found, as shown in Lavine and Jen (1991a). More recently, this model was modified (Jen and Lavine, 1992a) to allow the heat fluxes to vary with location (i.e., to allow x dependence), while the heat transfer coefficients for the various materials used were for uniform heat fluxes. For the case of uniform grinding power input, as was used in that study, this may not cause significant error. However, for the case of a triangular grinding power input, which may be more realistic for the grinding process (see, e.g., Kohli, 1993), this may cause significant error in the workpiece temperature prediction. This

will be shown later. An improved model is developed in the present study (also, see a preliminary study by Jen and Lavine, 1992b), which accounts for the effect of the heat flux variation along the grinding zone. With the aid of Duhamel's Theorem, the correct heat flux variations along the grinding zone are obtained numerically. The temperature and heat flux distributions along the grinding zone, and comparisons with previous theoretical results are presented.

Theoretical Analysis

The physical configuration and coordinate system for a typical grinding wheel and workpiece are shown in Fig. 1. The grinding zone is the region of length l and width b over which the wheel contacts the workpiece. The wheel and workpiece are shown moving in the same direction. This is termed "down" grinding. "Up" grinding, in which the wheel and workpiece are moving in different directions, is beyond the scope of the present study. However, with appropriate modifications, the present model could be used for up grinding. Some typical grinding parameters are shown in Table 1. There are two basic types of grinding: conventional and creep feed grinding. The major distinguishing features of creep feed grinding are the larger depth of cut and the lower workpiece speed.

It is helpful to recognize that there are many grains on the grinding wheel, which cut into the workpiece with very high speed. Heat is generated in the vicinity of each grain as it moves through the grinding zone. Consider an individual grain moving through the grinding zone. Heat is generated at three locations: the grain/workpiece interface, the grain/chip interface, and the shear plane between the workpiece and chip. Generally speaking, the frictional heat generated at the grain/chip interface is relatively small in comparison to the total grinding power. This was implicitly indicated by Malkin and Anderson (1974). Hahn (1956) argued that most of the heat is generated at grain/workpiece interfaces due to the larger frictional rubbing force than the cutting force (which is responsible for heat generation at the shear plane). This is especially true when the depth of cut of an individual grain is small. However, when this depth of cut is larger, the heat generated at the shear plane may not be negligible. In the present model, due to the significant complexity of including the effect of the heat generated at the shear planes, all the heat is assumed to be generated at the grain/workpiece interface.

Contributed by the Heat Transfer Division for publication in the JOURNAL OF HEAT TRANSFER. Manuscript received by the Heat Transfer Division November 1993; revision received July 1994. Keywords: Conjugate Heat Transfer, Materials Processing and Manufacturing Processes, Moving Boundaries. Associate Technical Editor: Y. Jaluria.

The heat generated at a grain/workpiece interface (q''_{grind}) conducts into either the workpiece or the abrasive grain. Thus,

$$q''_{\text{grind}}(x) = q''_{\text{wg}}(x) + q''_g(x) \quad (1)$$

where $q''_{\text{wg}}(x)$ is the heat flux into the workpiece at the grain location and $q''_g(x)$ is the heat flux into the grain.

Of the heat that conducts into the workpiece, (i.e., q''_{wg}), some remains in the workpiece and some is removed by convection to the grinding fluid. If it is assumed that the heat that conducts into the workpiece at a particular x location ($q''_{\text{wg}}(x)$) either remains in the workpiece or is removed by the fluid in the vicinity of that same location (see Jen, 1993, for detail), then:

$$q''_{\text{wg}}(x)A = q''_{\text{wb}}(x) + q''_f(x)(1 - A) \quad (2)$$

Here A is the fractional grain/workpiece contact area, $q''_{\text{wb}}(x)$ is the heat flux that remains in the workpiece, and $q''_f(x)$ is the heat flux into the fluid.

The basic approach used in the present study is first to develop thermal models for each heat transfer path (i.e., workpiece, grain and fluid) based on the assumption of uniform heat flux. (This assumption is later relaxed.) One result is a relationship between heat flux and temperature rise for each heat transfer path, of the form $h = q''/\theta$. The function h will be called a local heat transfer coefficient. These heat transfer coefficients were previously presented in Lavine and Jen (1991a, b), and will be briefly summarized here. Then the "conjugate" heat transfer problem, with varying heat fluxes, will be solved using Duhamel's Theorem.

Heat Transfer to Abrasive Grain, Workpiece, and Fluid. In order to solve the true problem with varying heat fluxes, the heat transfer coefficients for uniform heat fluxes are needed as a building block. The local grain, workpiece, and grinding fluid heat transfer coefficients due to a uniform heat flux input are given by (Lavine and Jen, 1991b):

$$h_g = \sqrt{\pi(k\rho c_p)_g v_s / 4x} f(\zeta) \quad (3)$$

where $\zeta(x) = (\pi\alpha_g x / A_0 v_s)^{1/2}$,

$$f(\zeta) = \frac{2\zeta}{\pi^{1/2} [1 - \exp(\zeta^2) \operatorname{erfc}(\zeta)]} \quad (4)$$

$$h_{\text{wb}}(x) = \sqrt{\frac{\pi(k\rho c_p)_w v_w}{4x}} \quad (5)$$

$$\bar{h}_{\text{wg}} = \frac{3}{4} \sqrt{\frac{\pi(k\rho c_p)_w v_s}{l_g}} \quad (6)$$

$$h_f(x) = \sqrt{\frac{\pi(k\rho c_p)_f v_s}{4x}} \quad (7)$$

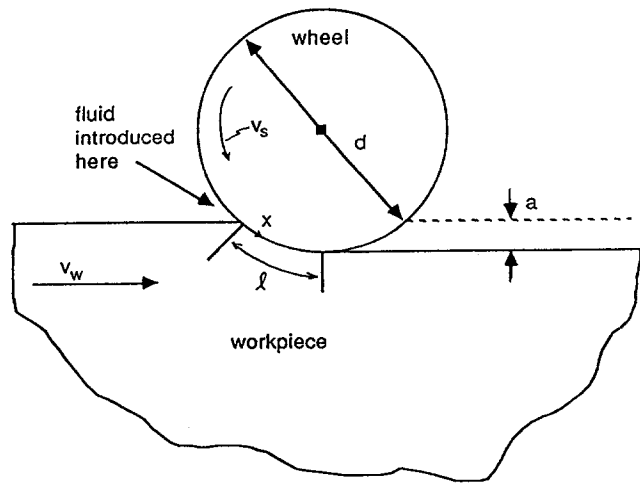


Fig. 1 Grinding geometry

For the grinding fluid heat transfer coefficient, slug flow is used throughout the present study rather than boundary layer flow, because it yields temperature predictions which agree better with experimental data. Note that this solution for h_f assumes that the fluid remains liquid. In reality, the fluid may boil under some conditions. This is discussed in more detail by Jen (1993).

Duhamel's Theorem. In early works (e.g., Malkin, 1974; Lavine and Jen, 1991a), a uniformly distributed heat flux into each component is assumed. However, as demonstrated in Lavine and Jen (1991a), the heat flux that enters each material is *not* uniform. A remedy is proposed by Jen and Lavine (1992a), in which they allowed the heat fluxes to vary with location while using the heat transfer coefficient for the uniform heat flux case. It will be demonstrated later that this approach does give a very good approximation of the temperature distribution when the grinding power input is uniformly distributed. However, this approach gives a very bad temperature prediction when the grinding power input is triangular. Very recently, a combined analytical and experimental study (Kohli, 1993) showed that a triangular grinding power input is more realistic under actual grinding conditions.

In order to allow the heat fluxes in the various models to vary with location, Duhamel's Theorem is applied. The general form of Duhamel's Theorem (Wylie and Barrett, 1982) for the surface temperature distribution is as follows:

$$\theta_s(x) = \int_0^x \frac{dq''(\xi)}{d\xi} \frac{1}{h(x-\xi)} d\xi \Big|_{\text{St.}} \quad (8)$$

Nomenclature

a = depth of cut
 A = fractional grain/workpiece contact area = A_g/A_{tot}
 A_0 = individual grain/workpiece contact area
 A_{tot} = grinding zone area = lb
 b = grinding zone depth
 C = a constant defined by Eq. (21)
 c_p = specific heat
 d = wheel diameter
 $f(\zeta)$ = function defined by Eq. (4)
 h = heat transfer coefficient for uniform heat flux
 k = thermal conductivity
 l = grinding zone length

l_g = width of individual grain heat source
 q'' = heat flux
 T_i = temperature before encountering grinding zone
 v_s = wheel velocity
 v_w = workpiece velocity
 x = distance from beginning of grinding zone
 α = thermal diffusivity
 ζ = $(\pi\alpha_g x / A_0 v_s)^{1/2}$
 θ = surface temperature rise relative to ambient temperature, i.e., $T - T_i$ (except for $\theta_{wg} = \bar{T}_{wg} - T_{wb}$)

ξ = dummy variable
 ρ = density

Subscripts

f = fluid
 i = nodal point index in the grinding zone
 g = grain
 grind = grinding power
 s = surface (except in v_s)
 St. = Stieltjes integral
 w = workpiece
 wb = workpiece background
 wg = workpiece under grain

Table 1 Typical grinding conditions ($v_s = 30$ m/s, $d = 200$ mm, $A = 0.01$, $l_g = 110$ μ m)

	v_w (mm/s)	a (mm)	$l = \sqrt{ad}$ (mm)
Conventional	100	0.005	1
Creep Feed	1	0.5	10

where St. means the Stieltjes integral, which incorporates the discontinuities of heat fluxes. The detailed formulations of temperature distributions for the different models are written below, with the assumption of discontinuities in heat fluxes only at $x = 0$. This assumption is modified in Jen (1993) to account for the occurrence of film boiling.

$$\theta_{wb,s}(x) = \int_0^x \frac{dq''_{wb}(\xi)}{d\xi} \frac{1}{h_{wb}(x-\xi)} d\xi + \frac{q''_{wb}(0)}{h_{wb}(x)} \quad (9)$$

$$\theta_{f,s}(x) = \int_0^x \frac{dq''_f(\xi)}{d\xi} \frac{1}{h_f(x-\xi)} d\xi + \frac{q''_f(0)}{h_f(x)} \quad (10)$$

$$\bar{\theta}_{wg,s}(x) = \int_0^x \frac{dq''_{wg}(\xi)}{d\xi} \frac{1}{\bar{h}_{wg}} d\xi + \frac{q''_{wg}(0)}{\bar{h}_{wg}(x)} = \frac{q''_{wg}(x)}{\bar{h}_{wg}} \quad (11)$$

$$\bar{\theta}_{g,s}(x) = \int_0^x \frac{dq''_g(\xi)}{d\xi} \frac{1}{h_g(x-\xi)} d\xi + \frac{q''_g(0)}{h_g(x)} \quad (12)$$

where the overbars denote averages underneath a single grain.

Note that all temperature rises must be zero at $x = 0$, from the boundary condition that the wheel, workpiece, and fluid temperatures are all equal to T_i at $x = 0$. This is automatically satisfied for $\bar{\theta}_{g,s}$, $\theta_{wb,s}$ and $\theta_{f,s}$, since $h_g(0)$, $h_{wb}(0)$, and $h_f(0)$ are all infinite. The requirement $\bar{\theta}_{wg,s}(0) = 0$ implies $q''_{wg}(0) = 0$. Then Eqs. (1) and (2) yield:

$$q''_g(0) = q''_{grind}(0) \quad (13)$$

$$q''_{wb}(0) + (1-A)q''_f(0) = 0. \quad (14)$$

Coupling the Models. The models for the wheel, fluid, and workpiece are now coupled by requiring that the surface temperatures match.

At a point on the workpiece surface that is not underneath a grain, the temperature rise is equal to the workpiece background temperature rise, $\theta_{wb,s}$, which must equal the fluid temperature rise, $\theta_{f,s}$:

$$\theta_{wb,s}(x) = \theta_{f,s}(x) \quad (15)$$

This leads to:

$$\int_0^x \frac{dq''_{wb}(\xi)}{d\xi} \frac{1}{h_{wb}(x-\xi)} d\xi + \frac{q''_{wb}(0)}{h_{wb}(x)} = \int_0^x \frac{dq''_f(\xi)}{d\xi} \frac{1}{h_f(x-\xi)} d\xi + \frac{q''_f(0)}{h_f(x)} \quad (16)$$

Now if $q''_{wb}(0)$ and $q''_f(0)$ are assumed to be nonzero, it can be shown that as $x \rightarrow 0$, the two integral terms in Eq. (16) approach zero faster than the other two terms. This implies $q''_{wb}(0)/h_{wb}(x) = q''_f(0)/h_f(x)$ for small x . The interested readers are referred to Jen (1993) for detailed derivations. In combination with Eq. (14) this yields $q''_{wb}(0) = q''_f(0) = 0$, so that the initial assumption of nonzero values is false. Then Eq. (16) becomes:

$$\int_0^x \frac{dq''_{wb}(\xi)}{d\xi} \frac{1}{h_{wb}(x-\xi)} d\xi = \int_0^x \frac{dq''_f(\xi)}{d\xi} \frac{1}{h_f(x-\xi)} d\xi \quad (17)$$

At a point on the workpiece surface that is beneath a grain, the grain temperature rise, $\bar{\theta}_{g,s}$, must equal the sum of the workpiece

background temperature rise and the individual grain temperature rise relative to the workpiece background temperature:

$$\bar{\theta}_{g,s}(x) = \theta'_{wb,s}(x) + \bar{\theta}_{wg,s}(x) \quad (18)$$

Similarly, this can be expressed as:

$$\int_0^x \frac{dq''_g(\xi)}{d\xi} \frac{1}{h_g(x-\xi)} d\xi + \frac{q''_{grind}(0)}{h_g(x)} = \int_0^x \frac{dq''_{wb}(\xi)}{d\xi} \frac{1}{h_{wb}(x-\xi)} d\xi + \frac{q''_{wg}(x)}{h_{wg}} \quad (19)$$

If $q''_{grind}(x)$ is assumed to be known, then Eqs. (1), (2), (17) and (19) are four equations that can be solved for the four unknown heat fluxes. In particular, these four equations can be combined into one integral equation for $q''_{wb}(x)$:

$$q''_{wb}(x) = \frac{A\bar{h}_{wg}}{1+(1-A)C} \left\{ \int_0^x \left(\left[\frac{dq''_{grind}(\xi)}{d\xi} - \frac{1}{A} \frac{dq''_{wb}(\xi)}{d\xi} (1+(1-A)C) \right] \frac{1}{h_g(x-\xi)} - \frac{dq''_{wb}(\xi)}{d\xi} \frac{1}{h_{wb}(x-\xi)} \right) d\xi + \frac{q''_{grind}(0)}{h_g(x)} \right\} \quad (20)$$

where:

$$C = \frac{h_f(x)}{h_{wb}(x)} = \frac{q''_f(x)}{q''_{wb}(x)} \quad (21)$$

where C is a constant. Note that Eq. (21) can be verified by using Eq. (17). It is worth noting that Eq. (20) is only valid when flow boiling doesn't occur. The readers are referred to Jen (1993) for detailed derivations when film boiling occurs.

Before giving details of the numerical procedure, a brief discussion of the differences between the present model and the previous models are discussed. It was pointed out by Lavine and Jen (1991a) that the true solution of this coupled heat transfer problem does not have uniform heat fluxes into each of the various materials. With some modifications, Jen and Lavine (1992a) allowed all the heat fluxes to vary with x , but they still used the heat transfer coefficients for uniform heat fluxes. It will be shown later that this approximate solution is quite accurate when $q''_{grind}(x)$ is uniform, but it is highly inaccurate when $q''_{grind}(x)$ is triangular. With the aid of Duhamel's Theorem, the present model correctly handles arbitrary heat flux variations. It is also worth noting that the triangular grinding power input may be more appropriate for the grinding process than the uniform grinding power input used previously (e.g., Kohli, 1993, and Ohishi and Furukawa, 1985). Therefore, this new model is more accurate and flexible, because it imposes less restrictive assumptions.

Numerical Procedure. It can be seen that the final expression of the governing equations, Eq. (20), is in the form of a Volterra integral equation. An attempt was made to solve it using a fixed point iteration method. However, the iterations did not always converge. An alternative method is employed that will now be described.

It is helpful first to recognize that all the heat transfer coefficients for the uniform heat flux case approach infinity as $x \rightarrow 0$. Thus, all kernels of the integral terms in Eq. (20) approach zero as $\xi \rightarrow x$. This reveals that we do not need information at $\xi = x$ for all integral terms. Therefore, if we use backward differences for the derivative $dq''_{wb}/d\xi$, we can march through the grinding zone, in the direction of increasing x , and solve explicitly for $q''_{wb}(x)$ from the left-hand side of Eq. (20). The only difficulty is that we cannot use backward differences at $x = 0$. But if we can determine the values of q''_{wb} at the first three discretized points after $x = 0$, we can solve this governing equation beyond these points without iteration. Bearing this concept in mind, the numerical procedure will now be presented as follows:

Table 2 Material properties and nondimensional parameters

	water-based	oil	Al ₂ O ₃	steel
k (W/m-K)	0.68	0.15	46	60.5
ρ (kg/m ³)	1000	820	4000	7854
c _p (J/kg-K)	4180	2000	770	434

1 In order to accelerate the convergence at the first three points, the first guess of $q''_{wb}(x)$ for these points is adopted from the previous approach (see Jen and Lavine, 1992a).

2 If we move the two terms on the right-hand side that are $q''_{wb}(x)$ dependent to the left-hand side, then the left-hand side of Eq. (20) is a function of $q''_{wb}(x)$ only and the right-hand side of the equation can be evaluated exactly. For the first three points, an iterative procedure is used (Jen and Lavine, 1992a) to solve for q''_{wb} , until the following convergence criterion is satisfied for the workpiece background temperature:

$$\epsilon = \frac{\max |\theta''_{wb,i}^{n+1} - \theta''_{wb,i}^n|}{\max |\theta''_{wb,i}^{n+1}|} < 10^{-6} \quad (22)$$

where i is the nodal point index in the grinding zone, and n is the iteration number.

3 With the values of $q''_{wb}(x)$ at these three points known, a second-order accuracy backward difference can be used for $dq''_{wb}/d\xi$ beyond those three points, so that Eq. (20) only has one unknown (i.e., $q''_{wb}(x)$). By marching along the grinding zone, all $q''_{wb}(x)$ can be calculated without further iteration.

4 With calculated $q''_{wb}(x)$, the other heat fluxes and temperatures can be calculated easily from Eqs. (1), (2), (21), and (9)–(12).

Grid convergence tests have been performed using three different grids for a case of creep feed grinding conditions, which is adopted from Ohishi and Furukawa (1985). As the grid size varies from 20001 to 40001, the maximum change in workpiece background temperature is less than 1.2 percent everywhere and less than 0.3 percent after $x = 3.58 \times 10^{-4}$ m. When the grid size varies from 40001 to 80001, the maximum change is less than 1 percent everywhere and less than 0.3 percent after $x = 1.57 \times 10^{-4}$ m, which is less than 1 percent of the total grinding zone. The error becomes smaller farther downstream. From the tests described above, 40001 grid points are sufficient for the present study.

Before giving the detailed results of the present model, an average grinding power is defined, for convenience, as follows:

$$q''_{tot} = \frac{1}{l} \int_0^l A q''_{grind}(x) dx \quad (23)$$

The reason for introducing Eq. (23) is that experimental results are usually reported in terms of q''_{tot} , that is, the total grinding power divided by the total grinding area.

Results and Discussion

In this section, this newly improved model will be used to give predictions of various temperatures and heat fluxes. The physical properties of abrasive grains (Al₂O₃), workpiece (steel), and grinding fluids (water-based or oil) are listed in Table 2. The grinding conditions, unless specifically stated, are the conditions listed in Table 1. The triangular grinding power input is used (unless otherwise stated). The average grinding powers used here are in the normal ranges of typical conventional and creep feed grinding conditions (Andrew et al., 1985). The workpiece material properties are taken to be those of plain carbon steel (see Table 2). The ambient temperature is taken to be 25°C for

water based grinding fluid and 40°C for oil, as explained in Lavine and Jen (1991a).

Comparison to Previous Results. The results of the present model will first be compared to the previous model (Jen and Lavine, 1992a) for creep feed grinding, using an aluminum oxide wheel and water-based grinding fluid. Figure 2 demonstrates the workpiece background temperature variation through the grinding zone, for the cases of uniform and triangular grinding power input. It can be seen from the figure that for the case of uniform grinding power input, the workpiece background temperature distribution for the present model is almost the same as the previous model. The maximum workpiece background temperature difference is less than 2°C. This close agreement is typical of all cases considered, which confirms the earlier statement that the approximate solutions presented by the previous model are quite accurate when $q''_{grind}(x)$ is uniformly distributed along the grinding zone. However, when the triangular grinding power input is used, the workpiece background temperatures predicted by these two models do not agree for x greater than about 2.0 mm. Furthermore, the previous model predicts that T_{wb} approaches T_i at the end of the grinding zone. This clearly unrealistic result indicates that the previous model cannot be used with a triangular grinding power input. This creates a problem in using the previous model, in light of the experimental observations by Kohli (1993) that a triangular grinding power input appears more accurately to simulate real grinding conditions.

It can be seen from the figure that the maximum workpiece background temperatures of the present model are approximately the same when using the two different grinding power inputs. This was true of all cases investigated. However, the workpiece background temperature distributions are vastly different for the two different shapes of grinding power input. For the uniform grinding power input case, the workpiece background temperature increases monotonically, and the maximum temperature always occurs at the end of the grinding zone. For the triangular grinding power input case, the temperature does not increase monotonically, and the maximum temperature occurs somewhere in the middle portion of the grinding zone. In this case, the maximum temperature occurs at about $x = 8$ mm (for a grinding zone length of 17.5 mm).

A comparison between the previous theoretical results and experimental measurements of the maximum workpiece background temperature was presented in Lavine and Jen (1991a). Since the present model agrees well with the previous model for prediction of the maximum workpiece background temperature, the comparison to experimental data would be essentially the

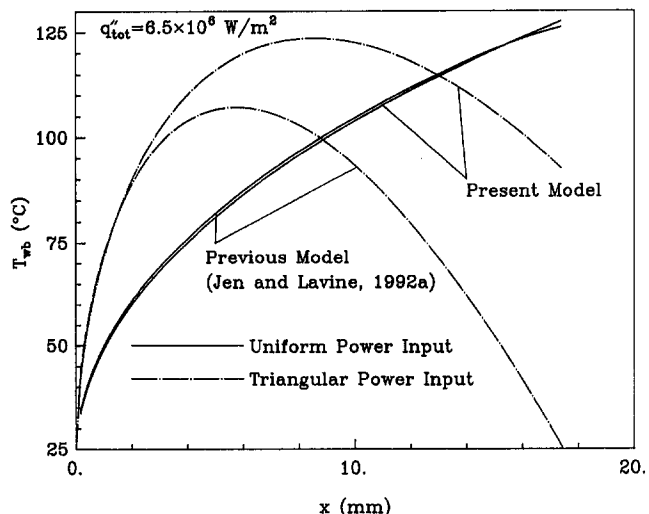


Fig. 2 Comparison to previous results: workpiece background temperature distribution

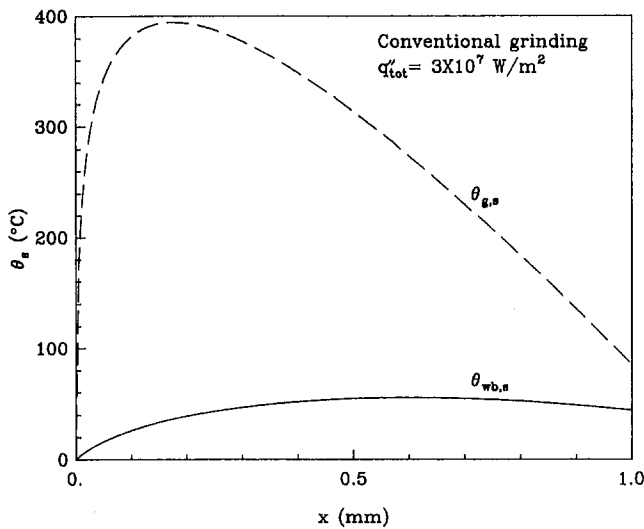


Fig. 3(a) Temperature distributions (triangular grinding power input, $q_{tot}'' = 3 \times 10^7 \text{ W/m}^2$, conventional grinding with water-based grinding fluid)

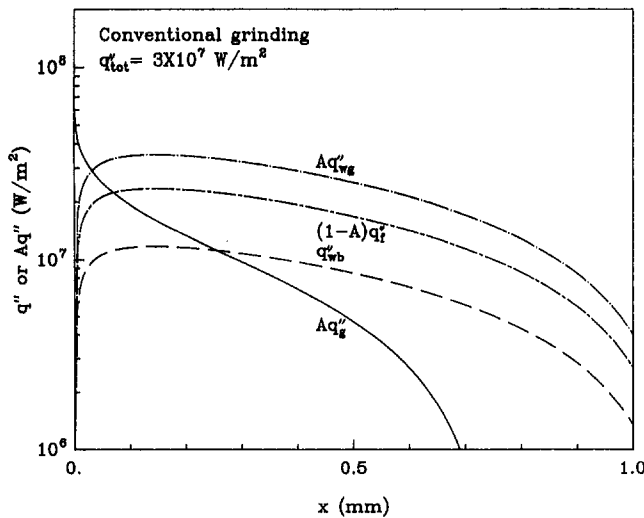


Fig. 3(b) Heat flux distributions (triangular grinding power input, $q_{tot}'' = 3 \times 10^7 \text{ W/m}^2$, conventional grinding with water-based grinding fluid)

same as in that earlier paper. To summarize, the theoretical model gives excellent agreement with experimental measurements for conventional grinding conditions (Yasui and Tsukuda, 1983). For creep feed grinding conditions (Ohishi and Furukawa, 1985), the model agrees well with experimental data when oil is used as the grinding fluid. However, the agreement is worse when water-based grinding fluid is used. There are several possible reasons for this discrepancy, for example, the effect of conduction in the direction of motion and the effect of shear plane heat generation. However, these will affect the temperature prediction for both water-based grinding fluid and oil. The true reasons for this discrepancy are still unresolved. Interested readers are referred to Jen (1993) for a detailed discussion.

Conventional Grinding Conditions. One example will be given to demonstrate the temperature and heat flux distributions along the grinding zone under conventional grinding conditions (see Table 1).

Figure 3(a) demonstrates the temperature distributions along the grinding zone for a case where film boiling does not occur. A triangular grinding power input with the average grinding power input of $3 \times 10^7 \text{ W/m}^2$ is used, which is specially chosen so that film boiling does not occur. It is clearly seen from the figure that the grain surface temperature rise, $\theta_{g,s}$, increases very

rapidly near the beginning of the grinding zone, and reaches its maximum value of 392°C at $x = 0.18 \text{ mm}$. The grain temperature rise decreases smoothly after the maximum temperature is reached. The workpiece background surface temperature rise, $\theta_{wb,s}$, is much lower than the grain surface temperature rise, $\theta_{g,s}$, throughout the grinding zone. A maximum workpiece background temperature rise of 56°C is reached at $x = 0.6 \text{ mm}$. Experiments by Yasui (1984) show that the workpiece background temperature peaks in the middle of the grinding zone, which agrees qualitatively with the present model.

Figure 3(b) shows the heat flux distributions along the grinding zone. The heat fluxes q_g'' and q_{wg}'' are usually two orders of magnitude larger than q_{wb}'' and q_f'' . This is because these heat fluxes occur over the small contact area of a grain (see Eqs. (1) and (2)). In order to give a clearer picture of the energy partition, two curves for Aq_{wg}'' and Aq_g'' are demonstrated instead of q_{wg}'' and q_g'' . These two heat fluxes (Aq_{wg}'' and Aq_g'') are per unit area of the grinding zone, rather than per unit area of actual contact. Similarly, $(1-A)q_f''$ is used instead of q_f'' .

It can be noted from Eq. (2) that the curve for Aq_{wg}'' is equal to the sum of the curves of q_{wb}'' and $(1-A)q_f''$. A triangular grinding power input is used with its maximum at the beginning of the grinding zone. It has been shown in Eq. (13) that the grain

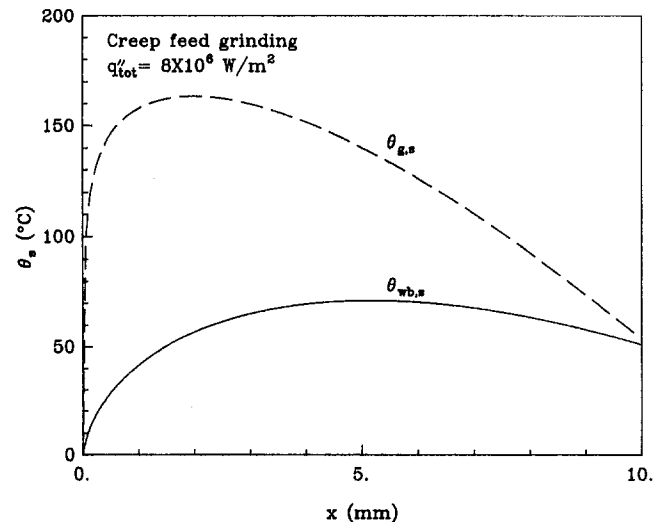


Fig. 4(a) Temperature distributions (triangular grinding power input, $q_{tot}'' = 8 \times 10^6 \text{ W/m}^2$, creep feed grinding with water-based grinding fluid)

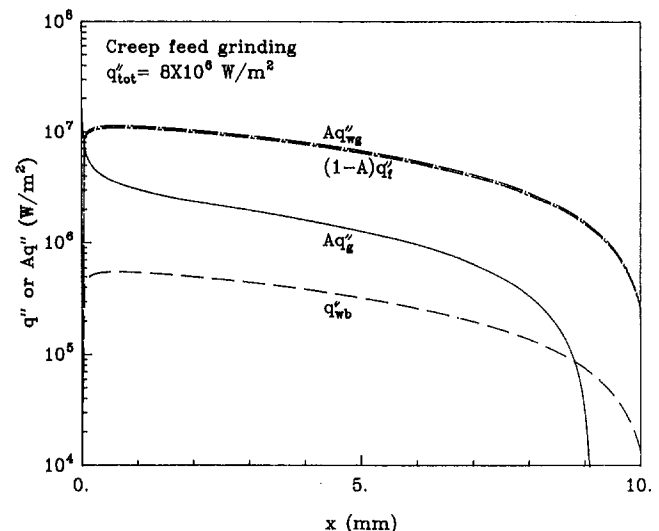


Fig. 4(b) Heat flux distributions (triangular grinding power input, $q_{tot}'' = 8 \times 10^6 \text{ W/m}^2$, creep feed grinding with water-based grinding fluid)

heat flux (q''_g) is equal to the grinding power input at $x = 0$. It can be seen that $Aq''_g = 6 \times 10^7 \text{ W/m}^2$ at $x = 0$ (two times the average grinding power input), and smoothly decreases. The grain heat flux, Aq''_g , becomes negative after about $x = 0.75 \text{ mm}$, which is not shown in the figure. This means that the heat generated at the grain/workpiece interface is totally removed by the workpiece along with additional heat from the grain. This can be explained as follows. The temperature underneath a grain reaches a maximum early in the grinding zone (see Fig. 3(a)) and then decreases. At some distance from the surface, the grain remains hot and therefore heat is transferred toward the surface. The workpiece cools faster than the grain due to such effects as convection to the fluid and its larger volume for heat diffusion. Therefore, the workpiece heat flux remains positive from the surface into the cooler region of the workpiece. Similar behavior was also found in an analysis presented by Guo and Malkin (1995). It can be seen that the heat that enters the workpiece (Aq''_{wg}) increases very rapidly near the beginning of the grinding zone, and reaches its maximum of $3 \times 10^7 \text{ W/m}^2$ at $x = 0.1 \text{ mm}$. After the maximum temperature point, Aq''_{wg} decreases throughout the grinding zone. Note that the heat that enters the workpiece (Aq''_{wg}) is either removed by the workpiece (q''_{wb}) or the grinding fluid ($(1 - A)q''_f$). It can be seen that the heat removed by the grinding fluid is about two times larger than the heat removed by the workpiece. In fact, 67 percent of the heat that enters the workpiece (or about 52 percent of q''_{tot}) is removed by the grinding fluid. It should be noted that the grinding fluid often undergoes film boiling under conventional grinding conditions, which greatly reduces the percentage of the heat removed by the grinding fluid (Lavine and Malkin, 1990).

Creep Feed Grinding Conditions. One example will be given here to show the temperatures and heat flux distributions along the grinding zone under creep feed grinding conditions. The grinding conditions are the typical creep feed conditions given in Table 1.

Figure 4(a) demonstrates the temperature distributions along the grinding zone for a case without film boiling. The average grinding power input is $8 \times 10^6 \text{ W/m}^2$. A triangular grinding power input is used with its maximum at the beginning of the grinding zone. The shapes of the temperature curves are similar to the conventional case shown in Fig. 3(a). Figure 4(b) shows the heat flux distributions along the grinding zone. In comparison to the example shown in Fig. 3(b) for conventional grinding conditions, the heat that enters the workpiece (Aq''_{wg}) is almost totally removed by the grinding fluid ($(1 - A)q''_f$) under creep feed grinding conditions, while a significant portion of the heat remained in the workpiece (q''_{wb}) under conventional grinding conditions. This was also confirmed experimentally by Shafto et al. (1975), in which they showed that most of the heat that enters the workpiece is removed by the grinding fluid.

Conclusions

A theoretical model has been developed to predict the temperature and heat flux distributions along the grinding zone. This model is developed successively by improving the earlier models (Lavine and Jen, 1991a, b; Jen and Lavine, 1992a), and eliminates many deficiencies encountered in the previous studies by many researchers. Several major conclusions can be made as follows:

1 Instead of assuming uniform heat flux into the workpiece, wheel, and fluid, the heat fluxes are allowed to vary with x by using Duhamel's Theorem.

2 As shown by Kohli (1993), a triangular grinding power input may be more appropriate under real grinding conditions. With triangular grinding power input, the present model demonstrates that the workpiece temperature distribution is distinctly

different from the workpiece temperature distribution when a uniform grinding power input is used.

3 For the case of triangular grinding power input, the maximum temperature is located somewhere in the middle, which agrees with experimental results (e.g., Kohli, 1993; Yasui, 1984), but the maximum temperature is located at the end of the grinding zone when a uniform grinding power is used. It is worth noting that if the maximum temperature occurs at the end of the grinding zone, this temperature could possibly be easily reduced by injecting grinding fluid at the end of the grinding zone.

4 The maximum workpiece temperature calculated for the uniform grinding power input case agrees very well with the same temperature predicted when a triangular grinding power is used.

5 In comparison to conventional grinding conditions, the heat removed by the grinding fluid is dominant under creep feed grinding conditions. This is in agreement with the results presented by Shafto et al. (1975).

Acknowledgments

The support of the National Science Foundation, General Motors, and General Electric is gratefully acknowledged.

References

- Andrew, C., Howes, T. D., and Pearce, T. R. A., 1985, *Creep Feed Grinding*, Holt, Rinehart, and Winston, New York, pp. 12–15.
- Carlslaw, H. S., and Jaeger, J. C., 1947, *Conduction of Heat in Solids*, Oxford University Press, London, United Kingdom.
- DesRuisseaux, N. R., and Zerkle, R. D., 1970a, "Thermal Analysis of the Grinding Process," *ASME Journal of Engineering for Industry*, Vol. 92, pp. 428–434.
- DesRuisseaux, N. R., and Zerkle, R. D., 1970b, "Temperature in Semi-infinite and Cylindrical Bodies Subjected to Moving Heat Sources and Surface Cooling," *ASME JOURNAL OF HEAT TRANSFER*, Vol. 92, pp. 456–464.
- Guo, C., and Malkin, S., 1995, "Analysis of Energy Partition in Grinding," *ASME Journal of Engineering for Industry*, Vol. 117, pp. 55–61.
- Hahn, R. S., 1956, "The Relation Between Grinding Conditions and Thermal Damage in the Workpiece," *Transactions of the ASME*, Vol. 78, pp. 807–812.
- Jen, T. C., and Lavine, A. S., 1992a, "Thermal Aspects of Grinding: The Effect of Flow Boiling," in: *Transport Phenomena in Materials Processing and Manufacturing*, ASME HTD-Vol. 196, pp. 91–98.
- Jen, T. C., and Lavine, A. S., 1992b, "Thermal Aspects of Grinding: An Improved Model of Heat Transfer to Workpiece, Wheel and Fluid," in: *Heat Transfer in Material Processing*, ASME HTD-Vol. 224, pp. 1–7.
- Jen, T. C., 1993, "Thermal Aspects of Grinding: Heat Transfer to Workpiece, Wheel and Fluid," Ph.D. Dissertation, MANE Department, UCLA.
- Kohli, S., 1993, "Energy Partition for Grinding With Aluminum Oxide and Cubic Boron Nitride Abrasive Wheels," Master's Thesis, Department of Mechanical Engineering, University of Massachusetts.
- Lavine, A. S., Malkin, S., and Jen, T. C., 1989, "Thermal Aspects of Grinding With CBN Wheels," *CIRP Annals*, Vol. 38, No. 1, pp. 557–560.
- Lavine, A. S., and Malkin, S., 1990, "The Role of Cooling in Creep Feed Grinding," *Int. J. Adv. Manuf. Technol.*, Vol. 5, pp. 97–111.
- Lavine, A. S., and Jen, T. C., 1991a, "Thermal Aspects of Grinding: Heat Transfer to Workpiece, Wheel, and Fluid," *ASME JOURNAL OF HEAT TRANSFER*, Vol. 113, pp. 296–303.
- Lavine, A. S., and Jen, T. C., 1991b, "Coupled Heat Transfer to Workpiece, Wheel, and Fluid in Grinding, and the Occurrence of Workpiece Burn," *Int. J. Heat Mass Transfer*, Vol. 34, No. 4/5, pp. 983–992.
- Lavine, A. S., 1991, "Thermal Aspects of Grinding: The Effect of Heat Generation at the Shear Planes," *Annals of the CIRP*, Vol. 40, No. 1, pp. 343–345.
- Malkin, S., and Anderson, R. B., 1974, "Thermal Aspects of Grinding. Part 1—Energy Partition," *ASME Journal of Engineering for Industry*, Vol. 96, pp. 1177–1183.
- Malkin, S., 1974, "Thermal Aspects of Grinding. Part 2—Surface Temperatures and Workpiece Burn," *ASME Journal of Engineering for Industry*, Vol. 96, pp. 1184–1191.
- Malkin, S., 1984, "Grinding of Metals: Theory and Application," *J. Applied Metalworking*, Vol. 3, No. 2, pp. 95–109.
- Ohishi, S., and Furukawa, Y., 1985, "Analysis of Workpiece Temperature and Grinding Burn in Creep Feed Grinding," *Bulletin of JSME*, Vol. 28, No. 242, pp. 1775–1781.
- Outwater, J. O., and Shaw, M. C., 1952, "Surface Temperatures in Grinding," *Transactions of ASME*, Vol. 74, pp. 73–86.
- Shafto, G. R., Howes, T. D., and Andrew, C., 1975, "Thermal Aspects of Creep Feed Grinding," *16th MTDR Conf.*, Manchester, United Kingdom, pp. 31–37.
- Snoeys, R., Maris, M., and Peters, J., 1978, "Thermally Induced Damage in Grinding," *CIRP Annals*, Vol. 27, No. 2, pp. 571–581.
- Wylie, C. R., and Barrett, L. C., 1982, *Advanced Engineering Mathematics*, McGraw-Hill, pp. 454–455.
- Yasui, H., and Tsukuda, S., 1983, "Influence of Fluid Type on Wet Grinding Temperature," *Bull. Japan Soc. of Prec. Engg.*, Vol. 17, No. 2, pp. 133–134.
- Yasui, H., 1984, "On Limiting Grinding Condition for Fluid Supply Effect," *Proceedings of 5th International Conference on Production Engineering*, Tokyo, pp. 58–63.